Chemical Engineering Journal 450 (2022) 138168

Contents lists available at ScienceDirect

Chemical Engineering Journal

journal homepage: www.elsevier.com/locate/cej

Synergistic photocatalytic treatment of aromatic hydrocarbons/NO_x mixtures over TiO_2: The activation and replenishment of lattice oxygen

Xiao Wang, Asad Mahmood, Guanhong Lu, Xiaofeng Xie *, Jing Sun *

The State Key Lab of High Performance Ceramics and Superfine Microstructure, Shanghai Institute of Ceramics, Chinese Academy of Sciences, 585 Heshuo Road, Shanghai 201899, China

ARTICLE INFO

Keywords:
Aromatic hydrocarbons (AHs)
Deactivation
NO_x
TiO_2
Lattice oxygen

ABSTRACT

The photocatalytic oxidation (PCO) mechanisms of single aromatic hydrocarbons/NO_x gases and the synergistic photocatalytic treatment of their mixtures over TiO_2 (anatase) are proposed by analyzing the evolution of adsorbed and gas-phase intermediates through in-situ FTIR and mass-spectroscopy. Photo-activated surface lattice oxygen of TiO_2 ($TiO_2(\cdot O_L)$) is found to be a strong oxidant for the PCO of both o-xylene and NO_x and their consumption led to the deactivation of photocatalysts. As an important coexist air pollutant, NO is firstly discovered as a helper for the persistent ring-opening and degradation of aromatics including o-xylene, toluene, styrene and benzene. NO_2, a PCO intermediate of NO, acts as a powerful oxidant for replenishing lattice oxygen of TiO_2, which guarantees the continuous generation of active $TiO_2(\cdot O_L)$ and prevents the deactivation of photocatalyst. With the introduction of NO, the PCO efficiency of o-xylene increases from ~65% to 100% and no performance decay of TiO_2 happens in 6 h. The existence of aromatics prevents the escape of toxic NO_2 into air and promotes the harmless transformation of NO into nitrite/nitrate ions and N_2. This work outlines the essential role of activation and replenishment of lattice oxygen in the PCO process by analyzing the synergistic and stable photocatalytic treatment of aromatic hydrocarbon/NO_x mixtures, which explores the practical potentiality of photocatalysis in air purification.

1. Introduction

As important by-products of the global industrialization process, the massive emission of gas phase pollutants caused several environmental problems like ozone and particulate matters, which have already been listed as the criteria air pollutants by the United States Environmental Protection Agency [1]. Due to the large emission and high ozone and PM2.5 formation potential, aromatic compounds including benzene, toluene and xylenes are among the most important hydrocarbons in air [2,3]. In recent years, the photocatalytic oxidation (PCO) technology has shown great potential in the elimination of gas pollutants due to its low cost, biosafety and low energy consumption. As one of the most commonly applied photocatalyst, TiO_2 has been widely studied in the PCO of various gas pollutants, including VOCs like aldehydes [4,5], aromatic hydrocarbons (AH) [6–8], alkenes and alkanes [9,10], as well as inorganic pollutants like NO_x and SO_2 [11–13], et al. In 2019, Chen el al. firstly proved the effectiveness of TiO_2 in preventing the formation of secondary organic aerosols (SOA) in the NO/m-xylene mixture, a typical reaction pair for the formation of SOA. The PCO technology shows great potential in indoor and outdoor air purification [14].

Under actual application scenarios, the co-existence of multiple gas pollutants and their interaction during PCO processes is one of the basic issues to be settled. The interaction between different pollutants may influence the performance of the photocatalyst or change the PCO mechanism of the target pollutants. Wang et al. studied the PCO of a mixed gas of benzene, p-xylene and toluene with P25 as the photocatalyst. Competitive adsorption and degradation happens between the pollutants and the PCO efficiency of every single pollutant decreased [15]. Synergistic degradation may also happen between different VOCs. Dong et al. found that the reaction between intermediates of formaldehyde and toluene could effectively lower the energy needed for the ring-opening of toluene and avoid the deactivation of the photocatalyst [16]. Aside from VOCs mixtures, NO_x and AHs also co-exist in various circumstances like automobile exhausts, industrial exhausts and gasoline vapor at gas stations [17–19] and has been reported as an important reaction pair for SOA formation [20,21]. Though lots of work has been done on the adsorption and PCO of NO_x and aromatics separately, [11,22–24] the study on the PCO of NO/aromatics mixtures is rare. The

* Corresponding authors.
E-mail addresses: xxfshcn@163.com (X. Xie), jingsun@mail.sic.ac.cn (J. Sun).

https://doi.org/10.1016/j.cej.2022.138168
Received 19 May 2022; Received in revised form 6 July 2022; Accepted 15 July 2022
Available online 19 July 2022
1385-8947/© 2022 Elsevier B.V. All rights reserved.

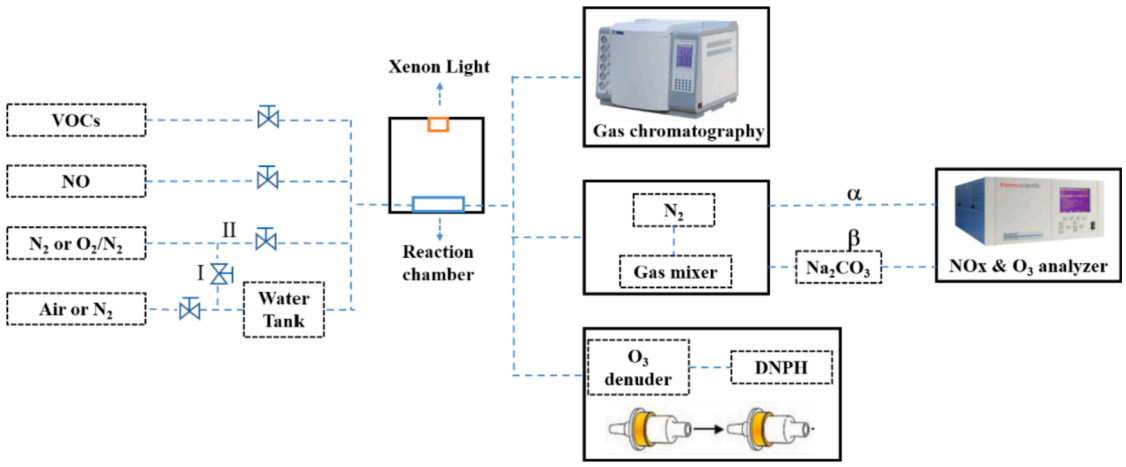

Scheme 1. Schematic diagrame of the gas curcuit during the PCO reactions.

interaction between both VOCs and NO with the surface of photocatalyst, and their mutual impact in reacting with oxidative radicals are essential for evaluating the application potential of TiO_2 photocatalyst in air purification.

The easy deactivation of TiO_2 and its composites, especially in the photocatalytic degradation of aromatic compounds, is another problem that severely diminish the commercial value of photocatalytic air purification [13]. Krichevaskaya et al. [25] observed the poison of TiO_2 during the PCO of styrene, which was mainly attributed to the relative slower degradation rates of the intermediates of styrene. An et al. further found the accumulation of benzyl intermediates as the main reason for the deactivation of TiO_2 during the PCO of styrene [26]. Similarly, the results by Dong et al. indicated that the occupation of active sites by ring-containing intermediates like benzaldehyde and benzoic acid leads to the deactivation of photocatalysts [27]. To solve the problem of catalyst deactivation, Rao et al. [28] used rGO to provide extra adsorption sites for the deposition of intermediates like o-tolualdehyde, phenyl, benzene, et al. and protect the active sites of TiO_2 from being occupied and maintain its high PCO activity toward o-xylene. However, the key factors affecting the ring-opening of aromatic hydrocarbons were still unclear and the problems of the massive generation and accumulation of intermediates were still unsolved. Dong et al. [29,30] explored the PCO of benzene, toluene and xylenes and figured out that the methyl substituent on benzene ring could activate the benzene ring and reduce the energy needed for ring-opening. They also found that ·OH, formed by the reaction between photo-excited holes and adsorbed water, act as an important ROS in the oxidation of AHs [30–32]. However, Su et al. [33] revealed that ·OH formed by single TiO_2 is not sufficient for the ring-opening of toluene. Abe et al. [34] studied the selective phenol production from the PCO of benzene and figured out that the direct oxidation of benzene by h^+ would result in undesired cleaved compounds, which confirmed the capability of h^+ in the ring-opening of aromatics. Despite all those efforts, most of the work today focus on the degradation of a single kind of pollutant, the roles of ROS, especially the role of ·OH and h^+ in the PCO of mixed pollutants are still unclear. In addition to oxidizing adsorbed water into ·OH, h^+ would also activate surface oxygen atoms into $TiO_2(\cdot O_L)$ [35], the role of which has been underestimated during the PCO reactions. Besides, most of the work only analyze the intermediates on the surface of photocatalysts, the monitoring over desorbed intermediates in gas phase are still difficult due to the lack of effective detection methods. The lack of these knowledge severely hindered the understanding of the deactivation-regeneration mechanism of TiO_2 photocatalyst in practical scenarios and therefore limits its commercial application in air purification.

Herein, we chose aromatic compounds including xylene, toluene, benzene and styrene as the target molecules to study the deactivation mechanism of TiO_2 photocatalysts and the PCO of aromatic hydrocarbon/NO_x mixtures due to their high ozone and SOA formation potential. Anatase TiO_2 with a band gap of 3.29 eV was applied as the photocatalysts in all the experiments (Fig. S1). In addition to on-line methods like *in-situ* Diffused Reflectance Infrared Fourier Transform Spectroscopy (DRIFTs) and off-line methods including electron paramagnetic resonance (EPR) and thermogravimetry-mass spectrometry (TG-MS), high-performance liquid mass spectrometry (HRLC-MS) coupled with 2,4-dinitrophenylhydrazine (DNPH) cartridge were applied to monitor both adsorbed and desorbed intermediates and reveal the PCO mechanism of o-xylene, NO and their mixtures. Synergistic PCO elimination of aromatic hydrocarbons/NO mixtures was observed, in which the PCO efficiency of o-xylene was significantly increased and the formation of toxic NO_2 was effectively depressed. The deactivation of TiO_2 was effectively avoided. Mechanistic insights into the mutual impact between o-xylene and NO are provided based on on-line and off-line characterizations. This research deepens the understanding on the photocatalytic mechanism of aromatic VOCs/NO_x mixtures and provide experimental basis for the practical application of TiO_2 in air purification.

2. Experimental section

2.1. Chemicals

Commercial titanium dioxide (TiO_2, Anatase, with particle size of 5 ~ 10 nm) was purchased from Taitan Corporation (General Reagent). Na_2CO_3 and $Na_2C_2O_4$ powder were purchased from Aladdin Industrial Corporation. NO (500 ppm), o-xylene (50 ppm), benzene (50 ppm), toluene (50 ppm) and N_2 standard gas were purchased from Shanghai Weichuang Standard Gas Analytical Technology Corporation. DNPH-silica cartridge (350 mg, 1 mL, DNWBOND) and ozone destructor cartridge (DNWBOND) were purchased from Shanghai ANPEL Laboratory Technologies Incorporation.

2.2. Photocatalytic Reactions:

To study the photocatalytic degradation procedure of typical VOCs (o-xylene, benzene and toluene) and NO_x, several photocatalytic reactions were carried out in a 20 cm × 10 cm × 1.5 cm reaction chamber covered by a quartz plate (Scheme 1). TiO_2 photocatalyst was firstly dispersed in ethanol through ball milling for 5 h and then coated on a 7.5 cm × 15 cm glass slide through scrape coating. The glass slides were then aged at room temperature for the complete evaporation of ethanol and then placed in the chamber. VOCs, NO_x and the balance gas (carrier gas) were mixed in a gas mixing tank and the mixture passed through the

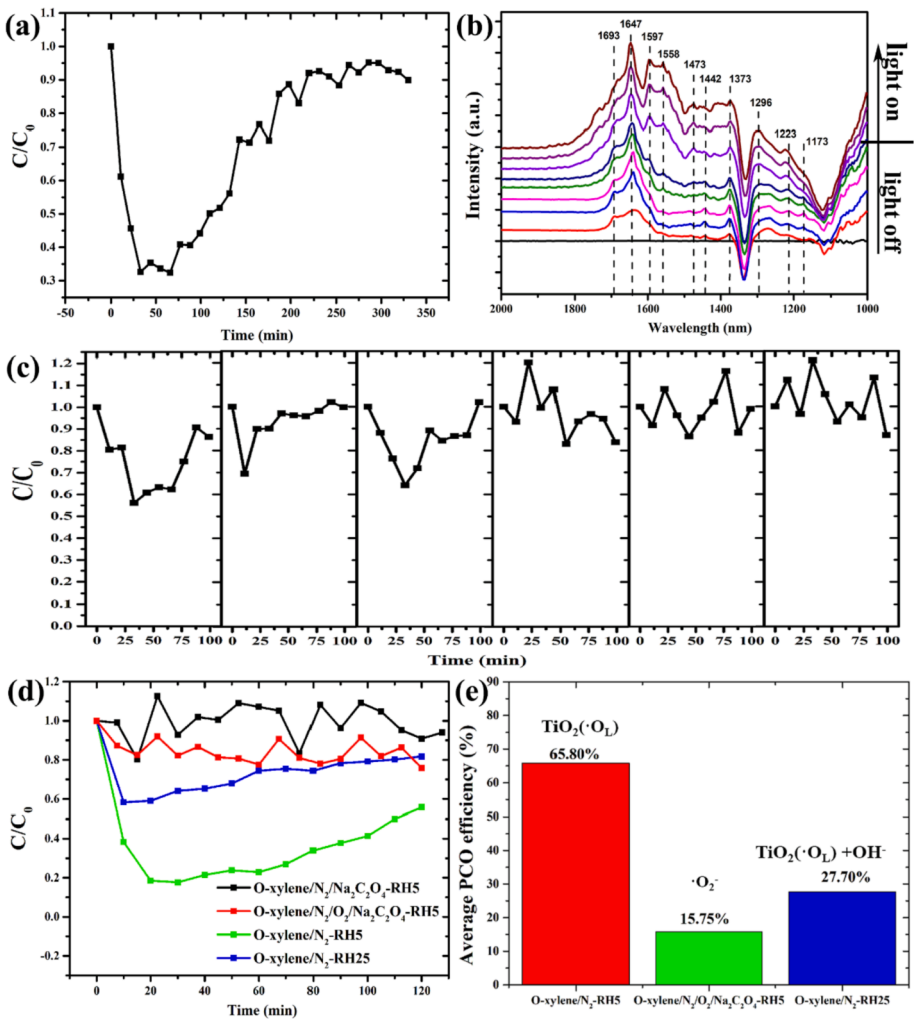

Fig. 1. (a) The PCO efficiency of o-xylene in o-xylene/ air; (b) The DRIFTs spectra of adsorbed products on the surface of TiO_2 during the PCO of o-xylene in the low-frequency region. The first spectrum is collected 3 min after the injection of pollutant gas and the following spectra are collected every 30 min; (c) the cyclic photocatalytic degradation of o-xylene in the o-xylene/ air system; (d) The PCO efficiency of o-xylene under different reaction conditions; (e) The contribution of various reactive radicals in the PCO of o-xylene.

reaction chamber with a fixed flow rate of 60 sccm. The concentration of o-xylene is set at 25 ppm to meet the detection limit of the analytical instruments. The humidity in the chamber was kept at ~58 %, ~25 % or ~5 % by controlling the percentage of carrier gas passing through the water tank or not (Route I and II in Scheme 1). In order to disclose the role of surface –OH groups, the photocatalyst was dehydrated in a vacuum oven at 80 °C for 5 h before being used. The concentration of VOCs and NO were regulated by adjusting the specific flow rates of the target gas and the balance gas (N_2) (Scheme 1). A 350 W Xenon light was placed 30 cm above the chamber as the light source. The cyclic degradation experiments were carried out on one sample for 6 times with each cycle lasting for 100 min. Between each cycle, the chamber was flushed with flow air and the photocatalyst was recovered by exposing to Xenon light in air for an hour. The concentration of VOCs was analyzed by a gas chromatography with a flame ionization detector (GC-FID, Beijing China Education Au-light Co., ltd., China). The adsorption and degradation efficiency η(100 %) was calculated according to *Eq. (1)*, in which C_0 and C stand for the initial concentration and the real-time concentration of VOCs. The mineralization efficiency (ME) was calculated through *Eq. (2)*, in which CO_{2_OUT} represents the concentration of CO_2 given by a GC-FID with a nickel catalyst accessory, which could convert low-level CO_2 into methane.

$$\eta(\%) = \left(1 - \frac{C}{C_0}\right) \times 100\% \tag{1}$$

$$ME(\%) = \frac{CO_{2_{OUT}}}{[C_0 \times 8 \times \eta(\%)]} \times 10000 \tag{2}$$

$$C = C_I * \frac{500 + v_{outlets}}{v_{outlets}} \tag{3}$$

A Thermo Scientific 42i Analyzer was applied to monitor the concentration of NO and NO_2. In order to meet the gas intake of the analyzer, N_2 with a flow rate of 500 sccm was used to dilute the mixed gas. The actual concentration of NO_x are calculated by *Eq. (3)*, where C_I represents the final results given by the instrument and $v_{outlets}$ stands for the flow rate at the outlets of the reaction chamber. As NO_2 and HONO are both recognized as NO_2 in the NO_x analyzer, a Na_2CO_3 denuder, which could capture HONO in the mixture, is applied to help determining the exact concentration of NO_2 and HONO (Route α and β in Scheme 1).

2.3. Detection of the products of photocatalytic reactions

The products in the gas phase were detected through a high-performance liquid chromatography mass spectrometry (HPLC-MS, Angilent 6460). According to previous reports, reactive oxygenated compounds (RCCs) were believed to dominate the mid-products of the photocatalytic reactions. 2,4-dinitrophenylhydrazine (DNPH)-silica cartridge coupled with ozone destructors were applied to collect the RCCs in the gas phase by forming derivatives with RCCs [14,36]. The derivatives were then extracted with 1 mL acetonitrile and analyzed

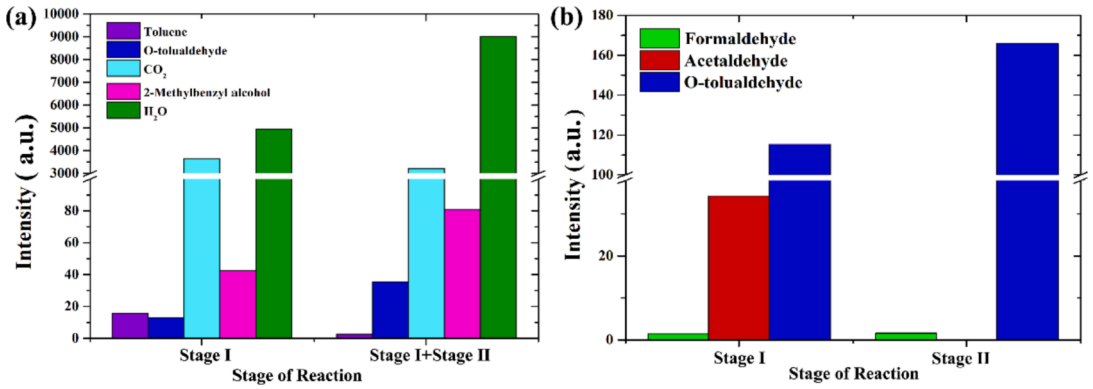

Fig. 2. Intermediates detected (a) on the surface of TiO_2 and (b) in the gas phase during different stages of the PCO reaction in o-xylene/air.

through HPLC-MS. In the purpose of understanding the reaction mechanism of NO_x, ion chromatography (Thermo Fisher, ICS-2100) was applied to detect the amount of NO_3^-, NO_2^- and NH_4^+ on the surface the photocatalyst. The analysis of the products on the surface of TiO_2 powder was carried out on a NETZSCH-STA449C thermal analysis mass spectrometer. The amounts of gaseous and adsorbed intermediates were qualitatively compared by calculating the area of corresponding HPLC-MS and TG-MS peaks.

In-situ DRIFTs (Hitachi Tracer 100 combined with mercury-cadmium-telluride detector) was applied to analyze the organics on the surface of TiO_2 powder in different reaction systems. The powder was placed in an in-situ reaction chamber (PIKE Technology) with two KBr windows and a glass window. The mixed gas mentioned above were injected into the chamber with a fixed flow rate of 60 sccm. After keeping the chamber in dark for 1.5 h to reach the adsorption–desorption equilibrium, an external Xenon light (CEAULIGHT TCX250) was applied as the light source during the photocatalytic reactions. FTIR spectra were collected every 3 min during the whole period to study the adsorption and PCO reaction of both VOCs and NO_x.

3. Results and discussion

3.1. The adsorption and photocatalytic oxidation of o-xylene

Before analyzing the interference between NO and o-xylene, the adsorption and PCO of single o-xylene and NO are studied. The effective adsorption of target molecules is the prerequisite for the PCO of gaseous pollutants. Therefore, we started with analyzing the adsorption behavior of o-xylene on TiO_2. As given by Fig. S2, TiO_2 shows promising performance in the adsorption and PCO of o-xylene with a saturated adsorption capacity of 1.02 mg/g. *In-situ* DRIFTs spectra is collected to monitor the adsorption of o-xylene on TiO_2 (Fig. 1b and S3). In addition to the bands assigned to aromatic ring (1442 cm^{-1}), methyl and ethyl groups (1373, 1223 cm^{-1}), aldehyde groups (1689, 1647 and 1173 cm^{-1}) (Table S1) are also observed, indicating the partial oxidation of o-xylene into benzyl aldehydes. The pre-oxidation has also been observed by Dong et al. [29] during the adsorption of o-xylene by SnO_2. Enhanced charge transfer was found between o-xylene and photocatalyst, and o-diphenol, o-phthalaldehyde and o-phthalic acid were observed as the dominant intermediates. When exposed to air, the coordination of surface Ti^{4+} sites in TiO_2 would be satisfied by the dissociative chemisorption of adsorbed water molecules, which results in the formation of Ti-OH groups on the surface of TiO_2. These Ti-OH groups could work as oxidative sites for the partial oxidation and adsorption of o-xylene into benzyl aldehydes [37], which consumes Ti-OH and results in negative bands observed at 3676 and 3723 cm^{-1} (the stretching vibration of isolated and associated surface Ti-OH species) [38]. To further confirm the role of Ti-OH groups in the adsorption of o-xylene, the adsorption capacity of o-xylene by TiO_2 in both water-free (RH ~ 5 %, noted as o-xylene/air-RH5) and humid (RH ~ 58 %, o-xylene/air-RH58) conditions are compared (Fig. S2). A vacuum heating treatment (80 °C, 5 h) is applied aforehand to remove most of the Ti-OH groups. An adsorption capacity of ~0.22 mg/g was obtained under water-free condition, much lower than the one under humid environment (~1.02 mg/g), confirming the importance of adsorbed water and –OH groups on the adsorption of o-xylene.

After starting the light irradiation, electrons and holes in TiO_2 are excited and migrated to the surface of TiO_2 to react with surface adsorbed O_2 and H_2O (or Ti-OH groups) and produce $\cdot O_2^-$ and ·OH radicals, respectively. Besides, h^+ could also combine with surface lattice oxygen to form active surface oxygen (noted as $TiO_2(\cdot O_L)$, *Eq. S1 ~ S4*) [35]. With the participation of these oxidative radicals, the degradation efficiency of o-xylene ($\eta_{o\text{-}xylene}$) by TiO_2 reaches 65 % in 30 min (Fig. 1a). However, deactivation of the photocatalyst happens after 75 min and $\eta_{o\text{-}xylene}$ drops to almost 0 in 270 min. Similar result can be observed in the cyclic experiments (Fig. 1c), in which the PCO activity of TiO_2 drops from 45 % to 0 in four cycles and remains at 0 from then. There are points at which C/C_0 are higher than 1, which might be related to the untimely degradation of o-xylene desorbed from the chamber wall and the photocatalyst.

In order to verify the role of the various oxidative radicals in the PCO of o-xylene, radical regulation experiments are carried out under different reaction atmosphere (Fig. 1d) and the types of predominant radicals are summarized in Table S2. An o-xylene/N_2/$Na_2C_2O_4$-RH5 reaction system is firstly built, in which $Na_2C_2O_4$ is applied as the h^+ scavenger to inhibit the activation of surface lattice oxygen ($TiO_2(O_L)$) into $TiO_2(\cdot O_L)$ and the formation of $\cdot OH^-$ radicals. O_2 and H_2O are cut off to avoid the generation of and $\cdot O_2^-$ radicals. Almost no degradation of o-xylene is observed in this system, confirming the key role of these radicals in the PCO process. The role of $TiO_2(\cdot O_L)$, $\cdot OH^-$ and $\cdot O_2^-$ radicals are then compared by testing the PCO efficiency of o-xylene in o-xylene/N_2-RH5, o-xylene/N_2/O_2/$Na_2C_2O_4$-RH5 and o-xylene/N_2-RH58. As given by Fig. 1e, $TiO_2(\cdot O_L)$ plays a key role in the degradation of o-xylene and enabled an average degradation efficiency of ~65.8 % (o-xylene/N_2-RH5). The key role of h^+ has also been discovered by Dong et al. in the PCO of m-xylene with Pt/TiO_2-R photocatalyst [30]. Instead of $TiO_2(\cdot O_L)$, they attributed the role of h^+ to the formation of ·OH radicals, which might be related to the fact that the pre-reduction of TiO_2 reduced the concentration of surface lattice oxygen and limited the generation of $TiO_2(\cdot O_L)$. EPR analysis (Fig. S4) reveals an increase in the concentration of oxygen vacancies (V_O) in TiO_2 after the PCO process in o-xylene/N_2-RH5, indicating that the oxidation of o-xylene by $TiO_2(\cdot O_L)$ would consume lattice oxygen and leave oxygen vacancies in TiO_2. An average degradation efficiency of 27.70 % is obtained with the introduction of water (o-xylene/N_2-RH25) and the deactivation of the photocatalyst happens in 20 min. Further increasing the relative humidity (58 % RH) led to the lower PCO efficiency of 25.07 % (Fig. S5). Unlike the adsorption process, water is unfavorable in the PCO of o-xylene for the

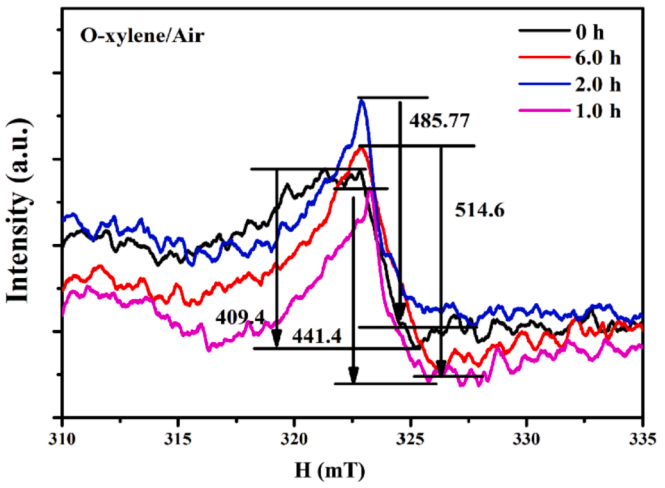

Fig. 3. The evolution of oxygen vacancies on TiO_2 in the degradation of o-xylene.

adsorbed H_2O would not only react with free h^+ to form $\cdot OH^-$ radicals, which competes with the generation of $TiO_2(\cdot O_L)$, but also occupy the active sites for the adsorption of o-xylene. As reported by Su et al [33], surface ·OH radicals generated by pristine TiO_2 were not as efficient as $TiO_2(\cdot O_L)$ for the ring-opening of toluene and would leave benzyl intermediates on the surface of TiO_2, which could explain the fast deactivation of TiO_2 in o-xylene/N_2-RH25 [33]. When only $\cdot O_2^-$ is reserved (o-xylene/N_2/O_2/$Na_2C_2O_4$-RH5), an average PCO efficiency of 15.75 % is achieved. Based on the above results, we can conclude that $TiO_2(\cdot O_L)$ plays a predominant role in the oxidative degradation of o-xylene.

To further understand the photocatalytic oxidation mechanism of o-xylene and the deactivation of photocatalyst, the evolution of intermediates both on the surface of TiO_2 and in the gas phase are analyzed. As given by the DRIFTs spectra in Fig. 1b, during the PCO of o-xylene, the band for benzene ring (~1597 cm^{-1}) splits into two bands at 1597 and 1558 cm^{-1}, together with the appearance of a new band at 1296 cm^{-1} (weak adsorption of benzyl aldehydes) and the increase in the peak for $-CH_2$ of benzyl species (1223 cm^{-1}), confirming the accumulation of both benzyl aldehydes and benzyl alcohols on the surface of TiO_2. TG-MS and HPLC-MS characterizations are then carried out to give the species and relative quantity of the intermediates (Fig. 2a and 2b). According to Fig. 1a, the deactivation of photocatalyst started at about 75 min and almost lost its activity in 6 h. Therefore, the species and amounts of intermediates generated during 0 ~ 75 min (Stage I) and 75 ~ 300 min (Stage II) of the PCO reaction are compared. The accumulation of adsorbed intermediates during Stage II (Fig. S6) is obtained by analyzing the differences between the organic matters detected after the entire reaction (Stage I + Stage II in Fig. 2a) and the ones obtained at the end of Stage I. As given by the TG-MS results (Fig. 2a), aside from water and CO_2, only first-generation intermediates like toluene, o-tolualdehyde and 2-methylbenzyl alcohol are detected on the surface of TiO_2 in Stage I. By using DNPH as the collector for gaseous intermediates [14,36], ring-opening products like acetaldehyde and formaldehyde are detected, suggesting the successive ring-opening of o-xylene during this stage (Fig. 2b). As the reaction proceeds (Stage II), the accumulation of o-tolualdehyde and 2-methybenzyl aldehyde continues, while a decrease happens in the amount of CO_2, which is in accordance with the decrease in the mineralization ratio of o-xylene (Fig. S7). At the same time, only a slight amount of formaldehyde is found in the gas phase while o-tolualdehyde is detected as the main product, indicating that the ring-opening ability of TiO_2 for aromatics is weakened and more benzyl aldehydes are released into the gas phase.

As discussed above, $TiO_2(\cdot O_L)$ is found to be a dominant radical during the oxidation of o-xylene and its consumption would increase the amount of $V_O^{\cdot\cdot}$ in TiO_2. Therefore, the evolution of the surface lattice oxygen during the PCO reaction is characterized through EPR. As shown by Fig. 3, the EPR intensity of $V_O^{\cdot\cdot}$ continuously increases from 409.4 to 514.6 in 6 h of the PCO reaction, confirming the consumption and untimely replenishment of lattice oxygen. These electron-rich $V_O^{\cdot\cdot}$ may work as trappers for free h^+ and result in the shortage of active $TiO_2(\cdot O_L)$, which is unfavorable for the photocatalytic activity of TiO_2 towards the PCO of o-xylene. Combining the weakened ring-opening ability of TiO_2 in stage II of the PCO process and the accumulation of oxygen vacancies, we can conclude that the untimely replenishment of lattice oxygen is one of the main reasons for the decreasing of photocatalytic efficiency and the accumulation of benzyl intermediates.

Based on the above analysis, the PCO mechanism of o-xylene could be proposed (Scheme 2). The surface of TiO_2 firstly capture o-xylene molecules and partially oxidized them into 2-methylbenzyl alcohol and o-tolualdehyde. Under the excitation of Xenon light, highly oxidative radicals including $\cdot O_2^-$, ·OH and $TiO_2(\cdot O_L)$ are generated and participate in the oxidative degradation of adsorbed species. During the initial stage of the PCO reaction, the fresh surface of TiO_2 provides enough $TiO_2(\cdot O_L)$ with strong oxidative ability for the fast and complete degradation of o-xylene (Route II in Scheme 2), which results in the high degradation efficiency of ~65 % and a CO_2 conversion ratio of 30 % (Fig. S7). Accordingly, instead of the aromatic species, ring-opening products like acetaldehyde, formaldehyde, CO_2, H_2O, ethylene and ethanol are found to be the dominant intermediates. The oxidation of o-xylene by $TiO_2(\cdot O_L)$ consumed lattice oxygen, which cannot be replenished in time by O_2 in air, resulting in the accumulation of $V_O^{\cdot\cdot}$ (Fig. 3) and the shortage of $TiO_2(\cdot O_L)$. The ring-opening process becomes the rate-determining procedure and Route I dominates, leading to the accumulation of benzyl intermediates. Both the accumulation of intermediates and the depletion of $TiO_2(\cdot O_L)$ result in the deactivation of the photocatalyst.

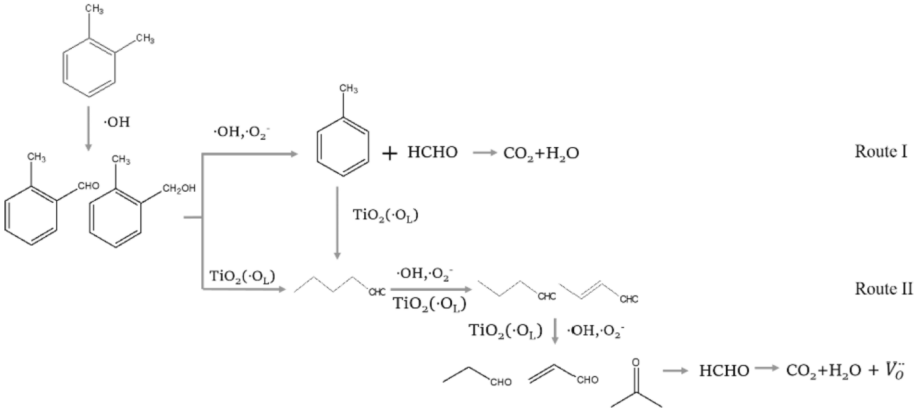

Scheme 2. The PCO mechanism of o-xylene in the o-xylene/ air reaction system.

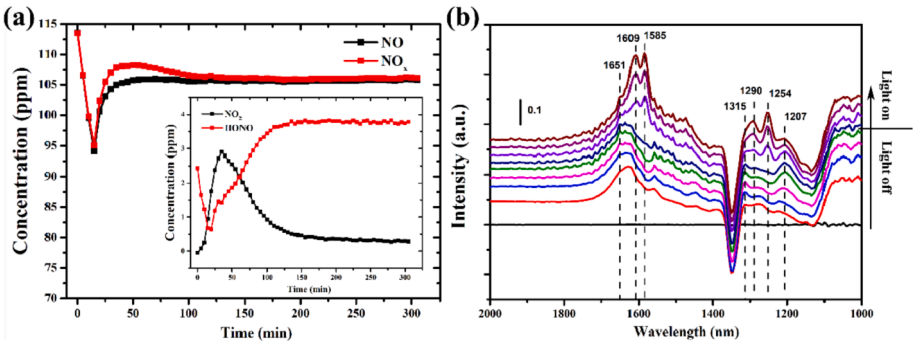

Fig. 4. (a) The concentration of NO, NO_x, NO_2 and HONO detected in the NO/air system with a Na_2CO_3 denuder; (b) DRIFTs spectra of adsorbed products on the surface of TiO_2 during the PCO of NO in the NO/air system. The first spectrum is collected 3 min after the injection of pollutant gas and the following spectra are collected every 30 min.

3.2. *The adsorption and PCO of NO with TiO_2*

As given by the DRIFTs results (Fig. 4b), partial oxidation happens during the adsorption of NO. The band at 1625 cm^{-1} is assigned to the δ(HOH) formed through the interaction between Ti-OH groups with nitrates. Bands and 1570, 1291 and 1207 cm^{-1} are assigned to monodentate nitrate and bidentate nitrite. Similar to the circumstance of o-xylene, negative peaks appear at 3670 and 3720 cm^{-1} during the absorption of NO (Fig. S8), indicating the partial oxidation of NO to NO_2^- and NO_3^- by surface oxidizing species like –OH and $TiOO^-$ [39]. After starting light irradiation, the degradation efficiency of NO (η_{NO}) firstly reaches 18.2 % in 20 min, and then drops to ~8.7 % in 40 min (Fig. 4a) and remains stable in the following 250 min. Both *in-situ* FTIR and ion chromatography analysis found NO_3^- as the dominant product (Fig. 4b and Table S3), while NO_2 is also detected during the PCO process (Eq. S5 ~ Eq. S11). In addition, the generation of oxygen vacancies during the PCO of NO is observed in the EPR results (Fig. S9), which reveals that the $TiO_2(\cdot O_L)$ radicals also participate in the oxidation of NO [24].

The key role of activated $TiO_2(\cdot O_L)$ during the photocatalytic decomposition of NO was firstly discovered by Pichat et al. in 1984 through a $N^{18}O$ isotope labeling method, by which activated surface ^{16}O from $Ti^{16}O_2$ would be detected in $N_2^{16}O$ products [40]. Ozensoy et al. further reported the PCO of NO goes through two separate pathways. On one hand, NO could be oxidized by ·OH and holes-activated $TiO_2(\cdot O_L)$

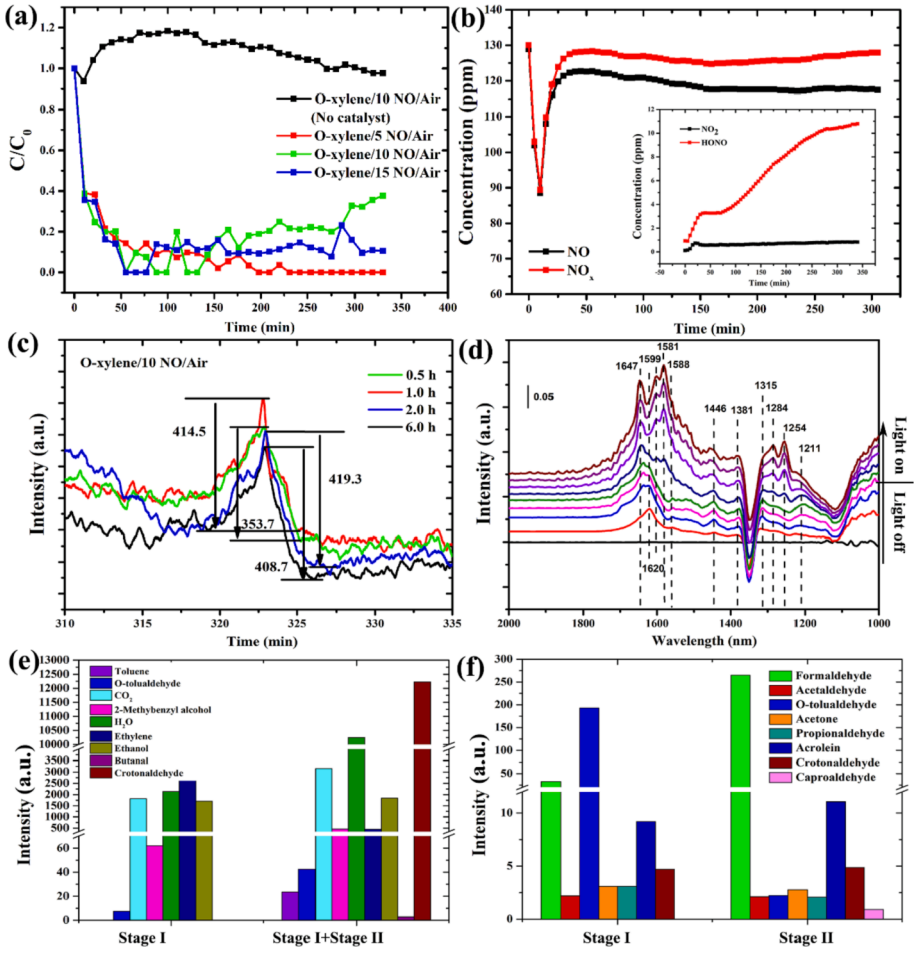

Fig. 5. (a)The PCO efficiency of o-xylene in o-xylene/NO/ air systems; (b) The concentration of NO, NO_x, NO_2 and HONO detected in the o-xylene/10 NO/ air system; (c) The evolution of oxygen vacancies in TiO_2 during the PCO of o-xylene/10 NO/ air; (d) The DRIFTs spectra of adsorbed products on the surface of TiO_2 during the PCO of the o-xylene/10 NO/ air system in the low-frequency region; The evolution of intermediates detected (e) on the surface of TiO_2 and (f) in the gas phase in the o-xylene/10 NO/air system.

into HNO_2, NO_2, NO_3^-, NO_2^- and HNO_3. On the other hand, $\cdot O_2^-$ would also participate in the reaction and oxidized NO into NO_2 and HNO_3 [35]. Combining with the PCO and *in-situ* DRIFTS results above, the PCO mechanism of NO could be proposed (Scheme S1). $TiO_2(\cdot O_L)$, ·OH and $\cdot O_2^-$ all participate in the oxidation of NO to form NO_2, HONO, NO_3^- and NO_2^-.

3.3. The synergistic PCO of aromatic hydrocarbon/NO_x mixtures

In order to understand the PCO mechanism of o-xylene/NO mixtures and the mutual impact between the two gases, NO with different concentrations are mixed with o-xylene (Fig. 4a). By introducing NO with a concentration of ~83 ppm (5 times the concentration of o-xylene, noted as o-xylene/ 5NO/ air), the degradation efficiency of o-xylene ($\eta_{o\text{-}xylene}$) increases to 100 % and remains stable for ~60 min. However, deactivation of the photocatalyst still happens after 130 min and $\eta_{o\text{-}xylene}$ drops from 100 % to ~65 %. When increasing the concentration of NO to ~167 ppm (o-xylene/ 10NO/ air), the degradation efficiency reaches 100 % in 200 min and no deactivation of the photocatalyst is observed in 330 min. Further increasing the concentration of NO does not result in an increase in the degradation efficiency accordingly, indicating that the impact of NO has approached saturation. The high stability of TiO_2 in the o-xylene/ 10NO/air system is also confirmed by cyclic degradation experiments (Fig. S10), which shows that the 100 % elimination of o-xylene remained for 5 cycles, much longer than that in the o-xylene/air system (Fig. 1c). Moreover, by introducing NO into o-xylene/air system in which the deactivation of TiO_2 has happened and $\eta_{o\text{-}xylene}$ has dropped from ~45 % to 30 %, $\eta_{o\text{-}xylene}$ goes back to ~55 % in ~110 min (Fig. S11), confirming that in addition to postponing deactivation, NO is also capable of re-generating TiO_2 photocatalyst.

In-situ DRIFTs spectra are firstly collected to clarify the positive effect of NO on the PCO degradation of o-xylene and the stability of TiO_2 (Fig. 5d). During the adsorption procedure, no obvious difference is observed in the intensity or position of bands assigned to o-xylene, benzyl aldehydes or benzyl alcohols compared with the DRIFTs spectra obtained in the o-xylene/ air reaction system. At the same time, the adsorption curves of o-xylene in the two reaction systems are basically the same (Fig. S12), indicating that the introduction of NO does not influence the adsorption of o-xylene. Differences between the two reaction systems are observed after starting the light irradiation. As given by Fig. 5d, the band for o-tolualdehyde (1646 and 1595 cm^{-1}) and bidentate nitrate (1585 cm^{-1}) appear after turning on the Xenon light, confirming the oxidation of both o-xylene and NO. The intensity of bands for benzoate species in the range of 1500 to 1370 cm^{-1} and the band for aromatic aldehyde at 1300 cm^{-1} all decrease with the introduction of NO, suggesting an alleviation in the accumulation of benzyl intermediates. The intermediates generated in the o-xylene/10 NO/air system are also analyzed through TG-MS and HPLC-MS. Unlike the o-xylene/air reaction system, ring-opening products like ethylene, ethanol, formaldehyde and acrolein are detected as the most abundant intermediates (Fig. 5e and 5f) during Stage I of the reaction. The differences between the o-xylene/air and o-xylene/ 10NO/air systems become more significant as the reaction progresses (Stage II). Compared with the o-xylene/air reaction system, more ring-opening products like formaldehyde, ethylene, ethanol, acetaldehyde, acetone, propionaldehyde, acrolein, methylglyoxal and crotonaldehyde are detected both on the surface of TiO_2 and in the gas phase (Fig. 5 and Fig. S13), while the amount of benzyl species remarkably decreases for the o-xylene/NO/air condition. The relative intensity of o-tolualdehyde detected in the gas phase of the o-xylene/ 10NO/ air system is almost one 80th of the o-xylene/air condition, which is in accordance with the *in-situ* FTIR results and confirms the positive role of NO in the ring-opening of o-xylene.

As discussed above in section 3.1, the fast replenishment of lattice oxygen and the consequent generation of sufficient $TiO_2(\cdot O_L)$ radicals is one of the key factors for the effective ring-opening and mineralization of o-xylene. Therefore, the variation of lattice oxygen during the PCO process in the o-xylene/ NO/air reaction system is also characterized (Fig. 5c). An increase in the concentration of oxygen vacancies from 353.7 to 414.5 in the o-xylene/NO/air system is observed during the first 60 min, which remains stable during the following 5 h, indicating that the consumption and replenishment of oxygen vacancies has reached an equilibrium during the reaction. Gaigneaux et al. studied the reaction of NO on VO_x/TiO_2 and found that NO_2 can efficiently replenish lattice oxygen, and at the same time being reduced to NO [41], which guarantees the continuous generation of highly oxidative $TiO_2(\cdot O_L)$ radicals. Based on the above results, we can hypothesis that the generation of NO_2 with promising ability in replenishing lattice oxygen might be the key reason for the high stability of the photocatalyst and the promoted PCO degradation of o-xylene. To prove the hypothesis, pre-reduced TiO_2 (TiO_2-R) with large amount of oxygen vacancies is synthesized by calcinating TiO_2 under hydrogen and applied as the photocatalyst for the degradation of o-xylene in the o-xylene/N_2-RH5, o-xylene/NO/N_2-RH5 and o-xylene/NO_2/N_2-RH5 systems. N_2 instead of air is used as the carrier gas to exclude the effects of O_2. As shown by Fig. S14, almost no degradation of o-xylene is observed in o-xylene/N_2-RH5 or o-xylene/NO/N_2-RH5, indicating that TiO_2-R cannot provide enough $TiO_2(\cdot O_L)$ radicals for the PCO of o-xylene. However, when NO_2 is introduced into the reaction system, a relatively high $\eta_{o\text{-}xylene}$ of ~70 % is obtained, which remains stable in 2 h. Considering that NO_2 alone cannot oxidize o-xylene under light irradiation (the o-xylene/10 NO_2/ air circumstance in Fig. S12), the role of NO_2 in promoting the PCO of o-xylene by TiO_2-R is confirmed. EPR analysis is also carried out to characterize the variation in oxygen vacancies. As shown by Fig. S15, the concentration of oxygen vacancies in TiO_2-R does not change much after the PCO reaction in o-xylene/N_2 and o-xylene/NO/N_2, while a significant reduction happens after the PCO process in o-xylene/NO_2/N_2, confirming the ability of NO_2 in oxidizing TiO_2-R and fill the oxygen vacancies. These supplemented lattice oxygens are then activated under light irradiation into $TiO_2(\cdot O_L)$ and participate in the oxidative degradation of o-xylene, which further proves the importance of $TiO_2(\cdot O_L)$ in the PCO of o-xylene.

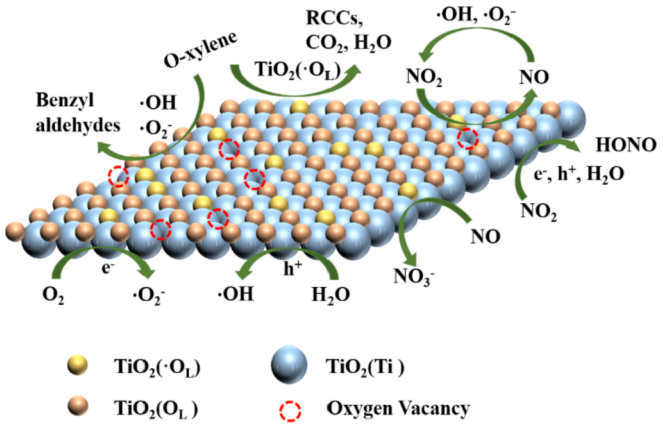

Scheme 3. The PCO mechanism in the o-xylene/NO/air reaction system.

In addition, the influence of o-xylene on the photocatalytic treatment of NO was also studied by characterizing the *N*-species formed during the PCO process of o-xylene/NO mixtures through on-line gas concentration tests and ion chromatography. Compared with the NO/air system, the formation of toxic NO_2 is depressed in the o-xylene/NO/air reaction system, while the generation of HONO is enhanced (Fig. 5b and Eq. S11). As given by Table S3, the amount of NO_3^- on the surface of TiO_2 decreases significantly in o-xylene/NO/air, while an increase happens in the amount of NO_2^- from 0.8 μg/ml (NO/air) to 218 mg/ml, in accordance with the decrease in bidentate NO_3^- observed in the *in-situ* FTIR results (Fig. 4d). Interestingly, the total amount of *N*-species on the surface of TiO_2 decreases, which is contradictory to the total *N*-balance and the changes in the concentration of gaseous NO_x mentioned above.

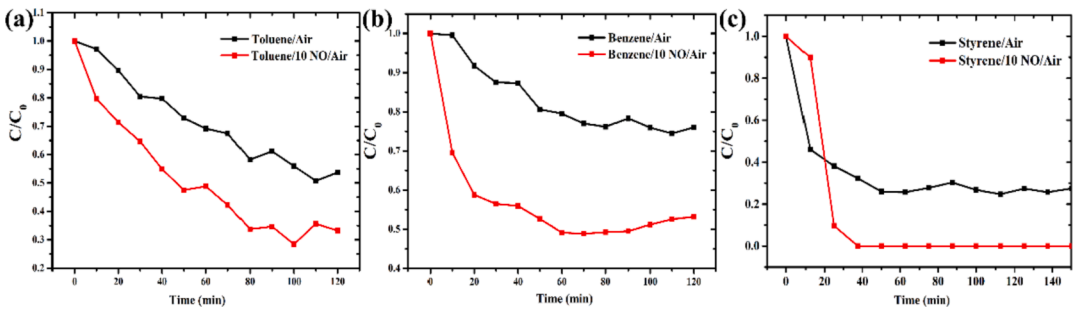

Fig. 6. (a) The PCO efficiency of toluene in the toluene/air and toluene/10 NO/ air system; (b) The PCO efficiency of benzene in the benzene/air and benzene/10 NO/ air system; (c) The PCO efficiency of styrene in the styrene/air and styrene/10 NO/ air system.

Considering the fact that no nitro-organics was detected neither on the surface of TiO_2 nor in the gas phase, the extra NO is reduced to N_2 with o-xylene acting as the reductant and achieve the harmless treatment of NO [42].

On the basis of the analysis above, the mechanism of the synergistic PCO of o-xylene/NO mixtures are proposed. During the adsorption process, both o-xylene and NO react with Ti-OH groups on the surface of TiO_2 to form aromatic aldehydes, nitrate and nitrite species. After starting the light irradiation, the oxidation of NO and o-xylene by the photo-induced radicals happens simultaneously (Scheme 3). On one hand, NO can react with $TiO_2(\cdot O_L)$ radicals and be directly oxidized to nitrate or nitrite species, which would absorb on the surface of TiO_2. On the other hand, the incomplete oxidation of NO by $\cdot OH^-$ or $\cdot O_2^-$ radicals would also lead to the formation of NO_2. As a strong oxidizer for the replenishment of lattice oxygen through the MvK reaction [43], NO_2 guarantees the generation of enough $TiO_2(\cdot O_L)$ radicals for the complete mineralization of o-xylene (Route II in Scheme S2), which postpone the deactivation of TiO_2. At the same time, toxic NO_2 is reduced to NO (or HONO with the existence of water, photo-excited electrons and holes, Eq. S11) [44] and part of the NO is transformed into N_2, realizing the environmental-friendly treatment of NO_x.

Aside from o-xylene, benzene, toluene and styrene are also important aromatic pollutants. The impact of NO on the PCO of these aromatic hydrocarbons are also characterized to verify the universality of NO in promoting the PCO of aromatic compounds. As shown in Fig. 6, the introduction of NO increases the degradation efficiencies of toluene, benzene and styrene from ~50 %, ~25 % and ~75 % to ~75 %, ~52 % and ~100 %, respectively. *In-situ* FTIR tests are also carried out to explore the promotion mechanism (Fig. S16 ~ S18). Similar to the case of o-xylene, decreases in the intensities of peaks for benzoate species (1550 ~ 1370 cm^{-1}) happen during the PCO of all the three aromatic hydrocarbons with the introduction of NO, revealing that the enhanced PCO efficiency also comes from the positive effect of NO in the ring-opening of aromatic pollutants.

4. Conclusion

In summary, the synergistic PCO treatment of o-xylene/NO mixtures over TiO_2 was analyzed and activated surface lattice oxygen ($TiO_2(\cdot O_L)$) was found to play a key role in the PCO reactions. The existence of NO improved the PCO degradation efficiency of o-xylene from ~65 % to 100 % and extend the time of highly efficient PCO from ~50 min to at least 6 h, while o-xylene could help with the transformation of NO into non-toxic N_2, NO_3^- and NO_2^-. TG-MS, HPLC-MS and *in-situ* DRIFTS analysis found ring-opening products like formaldehyde, acrolein and crotonaldehyde as the most abundant intermediates, confirming the enhanced ring-opening of o-xylene with the help of NO. NO_2, an intermediate of NO in PCO reactions, is found to act as a powerful oxidant for the replenishment of surface lattice oxygen and the continuous generation of active $TiO_2(\cdot O_L)$ radicals, which promote the ring-opening and mineralization of o-xylene. Such knowledge is quite essential for improving the stability and application value of TiO_2-based photocatalyst in eliminating flowing VOCs. Besides, as aromatic VOCs/NO_x is a typical atmospheric reaction pair for SOA formation, this work also helps in understanding the role of photocatalysts in impeding the formation of SOA. In future work, the design and optimization of anti-deactivation photocatalyst will be conducted to further promote the activation and replenishment of active surface lattice oxygen for the effective and stable elimination of air pollutants.

CRediT authorship contribution statement

Xiao Wang: Conceptualization, Investigation, Methodology, Formal analysis, Data curation, Funding acquisition, Writing – original draft. **Asad Mahmood:** Formal analysis, Investigation, Resources. **Guanhong Lu:** Formal analysis, Funding acquisition. **Xiaofeng Xie:** Formal analysis, Project administration. **Jing Sun:** Investigation, Validation, Funding acquisition, Resources, Project administration.

Declaration of Competing Interest

The authors declare that they have no known competing financial interests or personal relationships that could have appeared to influence the work reported in this paper.

Data availability

Data will be made available on request.

Acknowledgements

This work was financially supported by National Natural Science Foundation of China (41907303, 52072387), Natural Science Foundation of Shanghai (22ZR1471800), Shanghai Commission of Science and Technology Program (19DZ1202600, 20DZ1204100) and the State Key Laboratory Director Fund of SICCAS (Y9ZC0102).

Appendix A. Supplementary data

Supplementary data to this article can be found online at https://doi.org/10.1016/j.cej.2022.138168.

References

[1] Criteria Air Pollutants. https://www.epa.gov/criteria-air-pollutants.
[2] Y. Zhang, L. Xue, W.P.L. Carter, C. Pei, T. Chen, J. Mu, Y. Wang, Q. Zhang, W. Wang, Development of ozone reactivity scales for volatile organic compounds in a chinese megacity, Atmos. Chem. Phys. Discuss. 2021 (2021) 1–24.
[3] W.P.L. Carter, G. Heo, III D. R. C., S. Nakao, SOA FORMATION: CHAMBER STUDY AND MODEL DEVELOPMENT; Center for Environmental Research and Technology, College of Engineering, University of California: 2012.
[4] Q. Zeng, X. Xie, X. Wang, Y. Wang, G. Lu, D.Y.H. Pui, J. Sun, Enhanced photocatalytic performance of Ag@TiO_2 for the gaseous acetaldehyde photodegradation under fluorescent lamp, Chem. Eng. J. 341 (2018) 83–92.

[5] Q. Zeng, X. Wang, X. Xie, G. Lu, Y. Wang, S. Cheng Lee, J. Sun, TiO_2/TaS_2 with superior charge separation and adsorptive capacity to the photodegradation of gaseous acetaldehyde, Chem. Eng. J. 379 (2020), 122395.

[6] Z. Rao, X. Xie, X. Wang, A. Mahmood, S. Tong, M. Ge, J. Sun, Defect chemistry of Er^{3+}-doped TiO_2 and its photocatalytic activity for the degradation of flowing gas-phase VOCs, J. Phys. Chem. C 123 (19) (2019) 12321–12334.

[7] Q. Zeng, X. Wang, X. Xie, A. Mahmood, G. Lu, Y. Wang, J. Sun, Band bending of TiO_2 induced by O-xylene and acetaldehyde adsorption and its effect on the generation of active radicals, J Colloid Interface Sci 572 (2020) 374–383.

[8] M.S. Kamal, S.A. Razzak, M.M. Hossain, Catalytic oxidation of volatile organic compounds (VOCs) – a review, Atmos. Environ. 140 (2016) 117–134.

[9] X. Dai, Y. Wang, X. Wang, S. Tong, X. Xie, Polarity on adsorption and photocatalytic performances of N-GR/TiO_2 towards gaseous acetaldehyde and ethylene, Appl. Surf. Sci. 485 (2019) 255–265.

[10] A.H. Mamaghani, F. Haghighat, C.-S. Lee, Photocatalytic oxidation technology for indoor environment air purification: the state-of-the-art, Appl. Catal. B: Environ. 203 (2017) 247–269.

[11] J.Z. Bloh, A. Folli, D.E. Macphee, Photocatalytic NO_x abatement: why the selectivity matters, RSC Adv. 4 (86) (2014) 45726–45734.

[12] B. Wang, X. Li, S. Liang, R. Chu, D. Zhang, H. Chen, M. Wang, S. Zhou, W. Chen, X. Cao, W. Feng, Adsorption and oxidation of SO_2 on the surface of TiO_2 nanoparticles: the role of terminal hydroxyl and oxygen vacancy–Ti^{3+} states, Phys. Chem. Chem. Phys. 22 (18) (2020) 9943–9953.

[13] Y. Boyjoo, H. Sun, J. Liu, V.K. Pareek, S. Wang, A review on photocatalysis for air treatment: from catalyst development to reactor design, Chem. Eng. J. 310 (2017) 537–559.

[14] Y. Chen, S. Tong, J. Wang, C. Peng, M. Ge, X. Xie, J. Sun, Effect of titanium dioxide on secondary organic aerosol formation, Environ. Sci. Technol. 52 (20) (2018) 11612–11620.

[15] Z. Wang, X. Xie, X. Wang, A. Mahmood, H. Qiu, J. Sun, Difference of photodegradation characteristics between single and mixed VOC pollutants under simulated sunlight irradiation, J. Photochem. Photobiol., A 384 (2019), 112029.

[16] J. Li, R. Chen, W. Cui, X.a. Dong, H. Wang, K.-H. Kim, Y. Chu, J. Sheng, Y. Sun, F. Dong, Synergistic photocatalytic decomposition of a volatile organic compound mixture: high efficiency, reaction mechanism, and long-term stability, ACS Catal. (2020) 7230–7239.

[17] Correction for Ji et al., Reassessing the atmospheric oxidation mechanism of toluene. Proceedings of the National Academy of Sciences of the United States of America 2017, 114 (39), E8314.

[18] J. Li, W. Zhang, M. Ran, Y. Sun, H. Huang, F. Dong, Synergistic integration of Bi metal and phosphate defects on hexagonal and monoclinic $BiPO_4$: Enhanced photocatalysis and reaction mechanism, Appl. Catal. B: Environ. 243 (2019) 313–321.

[19] J.R. Odum, T.P.W. Jungkamp, R.J. Griffin, R.C. Flagan, J.H. Seinfeld, The atmospheric aerosol-forming potential of whole gasoline vapor, Science 276 (5309) (1997) 96–99.

[20] A. Zaytsev, A.R. Koss, M. Breitenlechner, J.E. Krechmer, K.J. Nihill, C.Y. Lim, J. C. Rowe, J.L. Cox, J. Moss, J.R. Roscioli, M.R. Canagaratna, D.R. Worsnop, J. H. Kroll, F.N. Keutsch, Mechanistic study of the formation of ring-retaining and ring-opening products from the oxidation of aromatic compounds under urban atmospheric conditions, Atmos. Chem. Phys. 19 (23) (2019) 15117–15129.

[21] Y. Wang, M. Hu, Y. Wang, J. Zheng, D. Shang, Y. Yang, Y. Liu, X. Li, R. Tang, W. Zhu, Z. Du, Y. Wu, S. Guo, Z. Wu, S. Lou, M. Hallquist, J.Z. Yu, The formation of nitro-aromatic compounds under high NO_x and anthropogenic VOC conditions in urban Beijing, China, Atmos. Chem. Phys. 19 (11) (2019) 7649–7665.

[22] J. Angelo, L. Andrade, L.M. Madeira, A. Mendes, An overview of photocatalysis phenomena applied to NO_x abatement, J. Environ. Manage. 129 (2013) 522–539.

[23] H. Li, H. Shang, Y. Li, X. Cao, Z. Yang, Z. Ai, L. Zhang, Interfacial charging-decharging strategy for efficient and selective aerobic NO oxidation on oxygen vacancy, Environ. Sci. Technol. (2019).

[24] Z. Hong, Z. Wang, X. Li, Catalytic oxidation of nitric oxide (NO) over different catalysts: an overview, Catal. Sci. Technol. 7 (16) (2017) 3440–3452.

[25] M. Krichevskaya, S. Preis, Gas-phase photocatalytic oxidation of styrene in a simple tubular TiO_2 reactor, J. Adv. Oxidation Technol. 6 (2) (2003).

[26] W. Zhang, G. Li, H. Liu, J. Chen, S. Ma, M. Wen, J. Kong, T. An, Photocatalytic degradation mechanism of gaseous styrene over Au/TiO_2@CNTs: relevance of superficial state with deactivation mechanism, Appl. Catal. B: Environ. (2020) 272.

[27] P. Chen, W. Cui, H. Wang, X.a. Dong, J. Li, Y. Sun, Y. Zhou, Y. Zhang, F. Dong, The importance of intermediates ring-opening in preventing photocatalyst deactivation during toluene decomposition, Appl. Catal. B: Environ. 272 (2020).

[28] Z. Rao, G. Lu, A. Mahmood, G. Shi, X. Xie, J. Sun, Deactivation and activation mechanism of TiO_2 and rGO/Er^{3+}-TiO_2 during flowing gaseous VOCs photodegradation, Appl. Catal. B: Environ. (2021) 284.

[29] Y. Sun, F. Dong, Unveiling the unconventional roles of methyl number on the ring-opening barrier in photocatalytic decomposition of benzene, toluene and o-xylene, Appl. Catal. B: Environ. 278 (2020).

[30] J. Zhang, K. Vikrant, K.H. Kim, F. Dong, Photocatalytic destruction of volatile aromatic compounds by platinized titanium dioxide in relation to the relative effect of the number of methyl groups on the benzene ring, Sci. Total Environ. 822 (2022), 153605.

[31] L. Yan, Q. Wang, W. Qu, T. Yan, H. Li, P. Wang, D. Zhang, Tuning $Ti^{\delta+}$-V_o-$Pt^{\delta+}$ interfaces over Pt/TiO_2 catalysts for efficient photocatalytic oxidation of toluene, Chem. Eng. J. 431 (2022).

[32] J. Li, K. Li, B. Lei, M. Ran, Y. Sun, Y. Zhang, K.-H. Kim, F. Dong, High-efficiency photocatalytic decomposition of toluene over defective InOOH: Promotive role of oxygen vacancies in ring opening process, Chem. Eng. J. 413 (2021).

[33] Q. Wu, J. Ye, W. Qiao, Y. Li, J.W. Niemantsverdriet, E. Richards, F. Pan, R. Su, Inhibit the formation of toxic methylphenolic by-products in photo-decomposition of formaldehyde–toluene/xylene mixtures by Pd cocatalyst on TiO_2, Appl. Catal. B: Environ. (2021) 291.

[34] O. Tomita, B. Ohtani, R. Abe, Highly selective phenol production from benzene on a platinum-loaded tungsten oxide photocatalyst with water and molecular oxygen: selective oxidation of water by holes for generating hydroxyl radical as the predominant source of the hydroxyl group, Catal. Sci. Technol. 4 (11) (2014) 3850–3860.

[35] M. Çağlayan, M. Irfan, K.E. Ercan, Y. Kocak, E. Ozensoy, Enhancement of photocatalytic NO_x abatement on titania via additional metal oxide NO_x-storage domains: interplay between surface acidity, specific surface area, and humidity, Appl. Catal. B: Environ. (2019) 118227.

[36] C.H. Ao, S.C. Lee, J.Z. Yu, J.H. Xu, Photodegradation of formaldehyde by photocatalyst TiO_2: effects on the presences of NO, SO_2 and VOCs, Appl. Catal. B: Environ. 54 (1) (2004) 41–50.

[37] F. Zhang, X. Zhu, J. Ding, Z. Qi, M. Wang, S. Sun, J. Bao, C. Gao, Mechanism study of photocatalytic degradation of gaseous toluene on TiO_2 with weak-bond adsorption analysis using in situ far infrared spectroscopy, Catal. Lett. 144 (6) (2014) 995–1000.

[38] Z. Wang, P. Ma, K. Zheng, C. Wang, Y. Liu, H. Dai, C. Wang, H.-C. Hsi, J. Deng, Size effect, mutual inhibition and oxidation mechanism of the catalytic removal of a toluene and acetone mixture over TiO_2 nanosheet-supported Pt nanocatalysts, Appl. Catal. B: Environ. (2020) 274.

[39] J. Wu, Y. Cheng, In situ FTIR study of photocatalytic NO reaction on photocatalysts under UV irradiation, J. Catal. 237 (2) (2006) 393–404.

[40] H. Courbon, P. Pichat, Room-temperature interaction of $N^{18}O$ with ultraviolet-illuminated titanium dioxide, J. Chem. Soc., Faraday Trans. 1 F 80 (11) (1984) 3175–3185.

[41] F. Bertinchamps, M. Treinen, N. Blangenois, E. Mariage, E. Gaigneaux, Positive effect of NO on the performances of VO_x/TiO_2-based catalysts in the total oxidation abatement of chlorobenzene, J. Catal. 230 (2) (2005) 493–498.

[42] L. Liao, S. Heylen, S.P. Sree, B. Vallaey, M. Keulemans, S. Lenaerts, M.B. J. Roeffaers, J.A. Martens, Photocatalysis assisted simultaneous carbon oxidation and NO_x reduction, Appl. Catal. B: Environ. 202 (2017) 381–387.

[43] F. Bertinchamps, M. Treinen, P. Eloy, A.M. Dos Santos, M.M. Mestdagh, E. M. Gaigneaux, Understanding the activation mechanism induced by NO_x on the performances of VO_x/TiO_2 based catalysts in the total oxidation of chlorinated VOCs, Appl. Catal. B: Environ. 70 (1–4) (2007) 360–369.

[44] S.K. Beaumont, R.J. Gustafsson, R.M. Lambert, Heterogeneous photochemistry relevant to the troposphere: H_2O_2 production during the photochemical reduction of NO_2 to HONO on UV-illuminated TiO_2 surfaces, Chemphyschem 10 (2) (2009) 331–333.